Supplementary Information (SI) for Dalton Transactions.

Electronic Supplementary Information

Constructing $Ni(OH)_2$ nanosheets on nickel foam electrode for efficient electrocatalytic ethanol oxidation

Shasha Ma, Di Chen, Zhaobin Ye, Yuanlong Wang, Jie Xu and Jianyong Zhang*

Sun Yat-Sen University, MOE Laboratory of Polymeric Composite and Functional Materials, School of Materials Science and Engineering, Guangzhou 510275, China. E-mail: zhjyong@mail.sysu.edu.cn.

Experimental section

Materials and characterization

Nickel foam (1.5 mm thickness) was procured from commercial source and cut into 1 cm × 1.5 cm. All materials and solvents were used without further purification unless otherwise specified. Hydrochloric acid (HCl, 36~38 wt.%) was diluted to 3 mol L^{-1} to remove the oxide layer from the nickel foam. Scanning electron microscopy (SEM) of the self-supporting NF electrodes was tested on a ZEISS Gemini 500 field emission scanning electron microscope (working voltage 10 kV, working current 10 μA). TEM were conducted on a Tecnai G2 F30 S-Twin transmission electron microscope. Samples were prepared by dispersing in EtOH upon sonication and placing on top of the carbon grid. X-ray diffraction (XRD) patterns were obtained on a MiniFlex600 instrument using Cu Kα (λ = 0.15468 nm) as the radiation source, and the scanning rate is 10 degrees per minute. Fourier transform infrared (FT-IR) spectra were recorded using a Thermo Fisher Nicolet iS10 spectrometer with KBr pellets. ^{1}H NMR spectra were acquired on a Bruker AVANCE AV 400 MHz spectrometer. *In-situ* Raman spectra were recorded using an XploRA PLUS instrument (Horiba) using a 532 nm laser in the region of 100 – 1000 cm^{-1}. The FU-NF electrode was assembled into a sealed spectroelectrochemical cell as the working electrode, Hg/HgO was used as the reference electrode, high-purity graphite as the counter electrode, and 1 mol L^{-1} KOH + 1 mol L^{-1} EtOH as the electrolyte. Amperometric measurements were conducted on a CHI660E electrochemical workstation (Chenhua) at open circuit potential and potential windows from 1.20 to 1.44 V vs. RHE, while in-situ Raman spectra were collected. Each Raman spectrum was collected with an integration time of 10 s and five times accumulations.

Electrochemical measurement

All the electrochemical measurements were performed in a three/two-electrode electrochemical workstation (CHI660E, Shanghai CH Instrument). A conventional three-electrode system was composed of Hg/HgO (saturated KCl solution) as reference electrode, a graphite rod as counter electrode and the as-obtained self-supported Nickel foam electrode directly as working electrode. The electrolyte was 1.0 mol L^{-1} KOH aqueous solution for OER and 1.0 mol L^{-1} KOH aqueous solution with 1.0 mol L^{-1} ethanol for EOR. Linear-sweep voltammogram curves and cyclic voltammogram were conducted at a scan rate of 50 mV s^{-1}. The potentials registered vs Hg/HgO as reference electrode were corrected for the uncompensated resistance using the formula $E_{\text{corrected}} = E_{\text{uncorrected}} - 95\% \times iR$, where R is the solution resistance obtained by electrochemical impedance spectroscopy (EIS), which was conducted at an AC voltage amplitude of 10 mV with frequencies ranging from 10^5 to 10^{-1} Hz. Moreover, all potentials were converted into potentials versus RHE utilizing the formula $E_{\text{RHE}} = E_{\text{corrected}} + E^0(\text{Hg/HgO}) + 0.059 \times \text{pH}$. Electrochemical double-layer capacitance (C_{dl}) was evaluated using different scan rates (20, 40, 60, 80, 100 mV s^{-1}) in the non-Faradaic region. The electrochemical stability was tested by chronoamperometric and chronopotentiometric measurements.

Preparation of NF electrodes

FU-NF was synthesized via one-step solvothermal method. Prior to preparation, Ni foam (2 cm× 2 cm ×1.5 mm) was ultrasonically cleaned for 15 min in 1 mol L^{-1} HCl to remove the surface oxide layer, and then the Ni foam was washed with deionized water and ethanol. Fumaric acid (116.1 mg, 1 mmol) was dissolved in 5 mL DMF under ultrasonication. The pretreated Ni foam was then immersed in this solution in a capped glass bottle, and heated at 80 °C for 2 h. After cooling to room temperature, the substrate was taken out and washed with deionized water. The resulting electrode was denoted as FU-NF. The electrochemical activation was conducted on a CHI660E electrochemistry workstation. The FU-NF electrode was activated by applying a constant potential of 1.4 V vs. RHE in 1.0 mol L^{-1} KOH + 1 mol L^{-1} ethanol. After test, FU-NF was washed with deionized water and ethanol three times. The resulting FU-NF electrode was under ultrasonication in ethanol and the powder FU-NF was separated by centrifugation.

BTC-NF and FDC-NF were prepared using 1,3,5-benzenetricarboxylic acid (210.1 mg, 1 mmol) and 2,5-furandicarboxylic acid (156.1 mg, 1 mmol), respectively, instead of fumaric acid. Phytate-NF and Tannate-NF were prepared using an aqueous solution of phytic acid (0.2 mol L^{-1}) and tannic acid (0.2 mol L^{-1}), respectively, instead of fumaric acid.

DMF-NF was prepared using the same solvothermal procedures as FU-NF but without adding fumaric acid. A piece of pretreated nickel foam (2 cm × 2 cm × 1.5 mm) was immersed in 5 mL of DMF in a capped glass bottle and heated at 80 °C for 2 h. After cooling to room temperature the nickel foam was washed with deionized water. The resulting electrode was referred to as DMF-NF. As for DIW-NF and AcO-NF, 5 mL deionized water and acetic acid solution were used instead of DMF.

For Bz-NF, benzoic acid (122.1 mg, 1 mmol) was dissolved in 5 mL of DMF under ultrasonication. The pretreated Ni foam was immersed in this solution, sealed in a capped glass bottle, and heated at 80 °C for 2 h. The resulting Ni foam was washed with deionized water, and dried, yielding the electrode denoted as Bz-NF.

Determination of CH_3COO^- by ^1H NMR

To determine the liquid products of the EOR, the electrolyte after chronopotentiometric measurement was detected by ^1H NMR. The concentration of the liquid product was calculated by comparing the integral area of the methyl group of CH_3COOK and CH_3CH_2OH. The standard curve was determined by a series of standard solutions of acetic acid in 1 mol L^{-1} EtOH aqueous solution.

Faradic efficiency was calculated through the equation

$$CH_3COO^- \ Faradic\ efficiency = \frac{4 \times F \times V \times \Delta c_{CH_3COO^-}}{Q} \times 100\%$$

where $\Delta c_{CH_3COO^-}$ is the change in CH_3COO^- concentration after electrolysis, F is the Faradaic constant (96485 C mol^{-1}), V is the volume of catholyte electrolyte (40 mL), and Q is the total electric charge passing the electrode during the electrolysis.

The hourly production rate of potassium acetate was calculated through the equation

$$CH_3COO^- \ yield = (\Delta c_{CH_3COO^-} \times V)/(t \times S)$$

where $\Delta c_{CH_3COO^-}$ is the change in CH_3COO^- concentration after electrolysis, V is the volume of catholyte electrolyte (40 mL), t is the reaction time, and S is the geometric area of working electrode.

Hybrid electrolysis

Hybrid electrolysis was evaluated using a two-electrode configuration using the electrode FU-NF (or NF) as the anode and the electrode CuO/CF (or CF) as the cathode separated by a Nafion 115 membrane. The concentrations of generated NH_3 (cathode) and acetate (anode) in the two-electrode system were quantified by ^1H NMR spectroscopy to calculate the Faradaic efficiency.

Mechanism of EOR

The mechanism of the ethanol oxidation to acetate occurring in an alkaline electrolyte is proposed to involve the following steps according to the literature.[11,38]

(1) Activation of $Ni(OH)_2$ to NiOOH: $Ni(OH)_2 + OH^- \rightarrow NiOOH + H_2O + e^-$;

(2) Oxidation of adsorbed ethanol: $CH_3CH_2OH + 4NiOOH + OH^- \rightarrow CH_3COO^- + 4Ni(OH)_2$

Fig. S1 Photographs of FU-NF in a capped bottle (left) before and (right) after the solvothermal process.

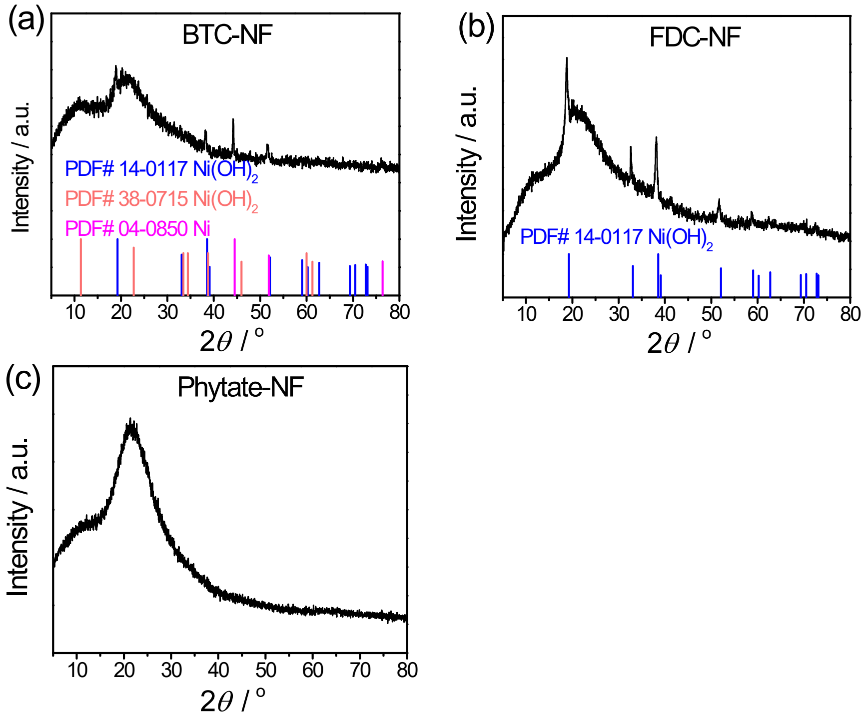

Fig. S2 XRD patterns of (a) powder BTC-NF, (b) powder FDC-NF and (d) powder Phytate-NF.

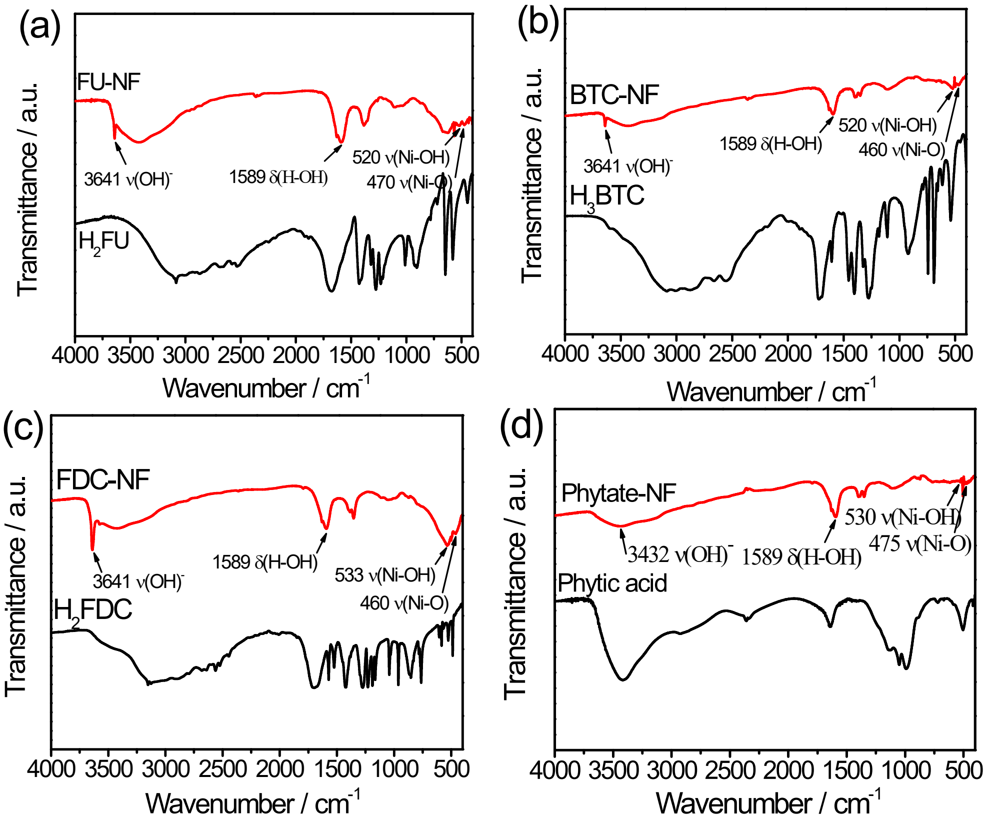

Fig. S3 FT-IR spectra of FU-NF, BTC-NF, FDC-NF and Phytate-NF.

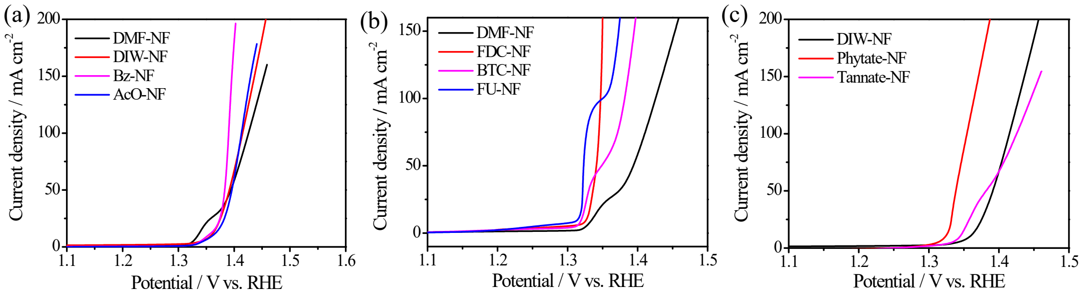

Fig. S4 (a) IR-corrected LSV curves of DMF-NF, DIW-NF, Bz-NF and AcO-NF toward EOR in 1.0 mol L^{-1} KOH and 1.0 mol L^{-1} EtOH, (b) LSV curves of DMF-NF, FDC-NF, BTC-NF and FU-NF, and (c) LSV curves of DIW-NF, Phytate-NF and Tannate-NF.

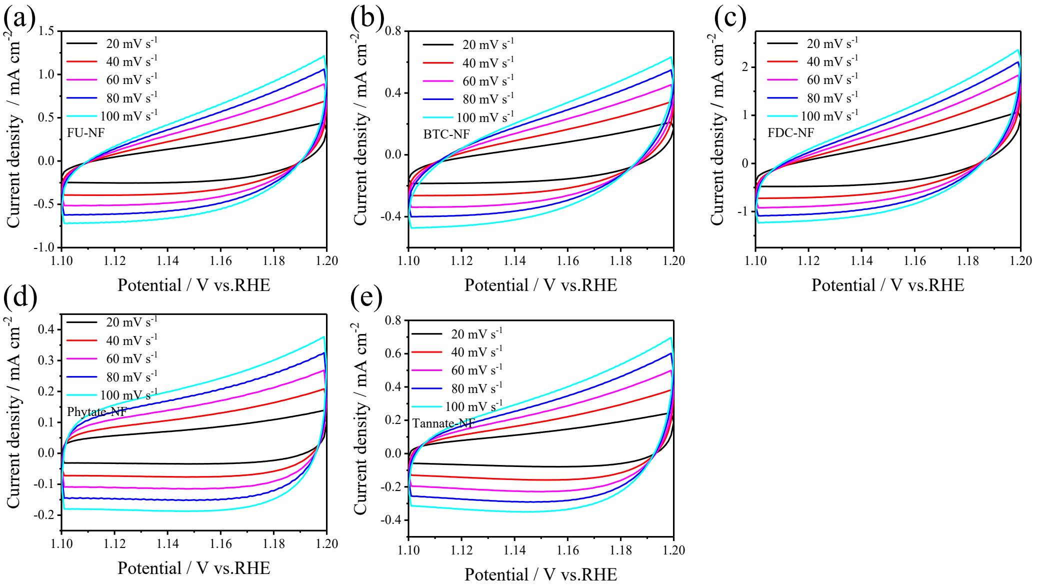

Fig. S5 CV curves of (a) FU-NF, (b) BTC-NF, (c) FDC-NF, (d) Phytate-NF and (e) Tannate-NF at different scan rates from 20 to 100 mV s^{-1} in the non-Faradic region.

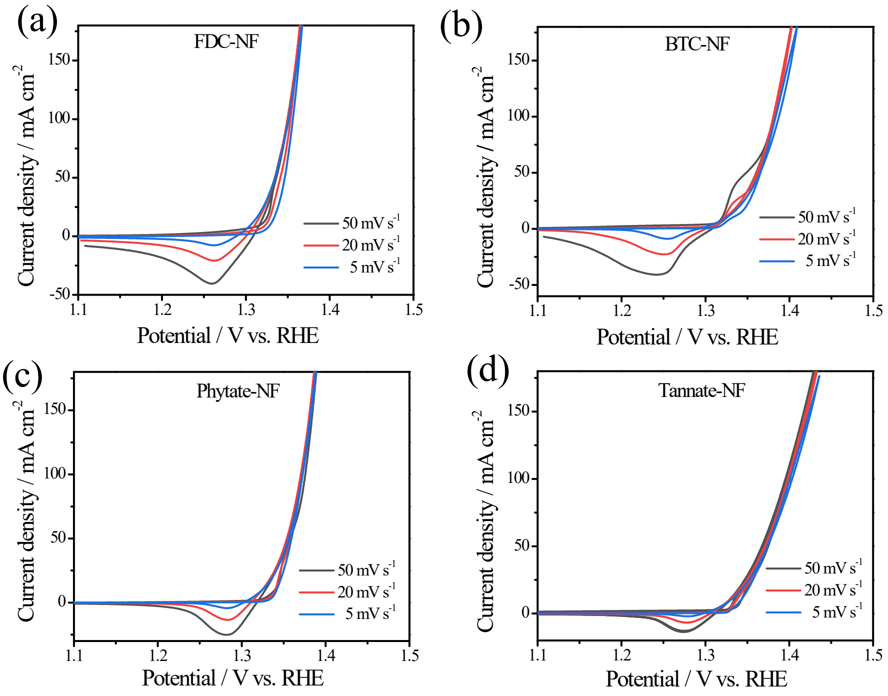

Fig. S6 CV curves of (a) FDC-NF, (b) BTC-NF, (c) Phytate-NF and (d) Tannate-NF in 1.0 mol L^{-1} KOH with 1.0 mol L^{-1} EtOH at different scan rates.

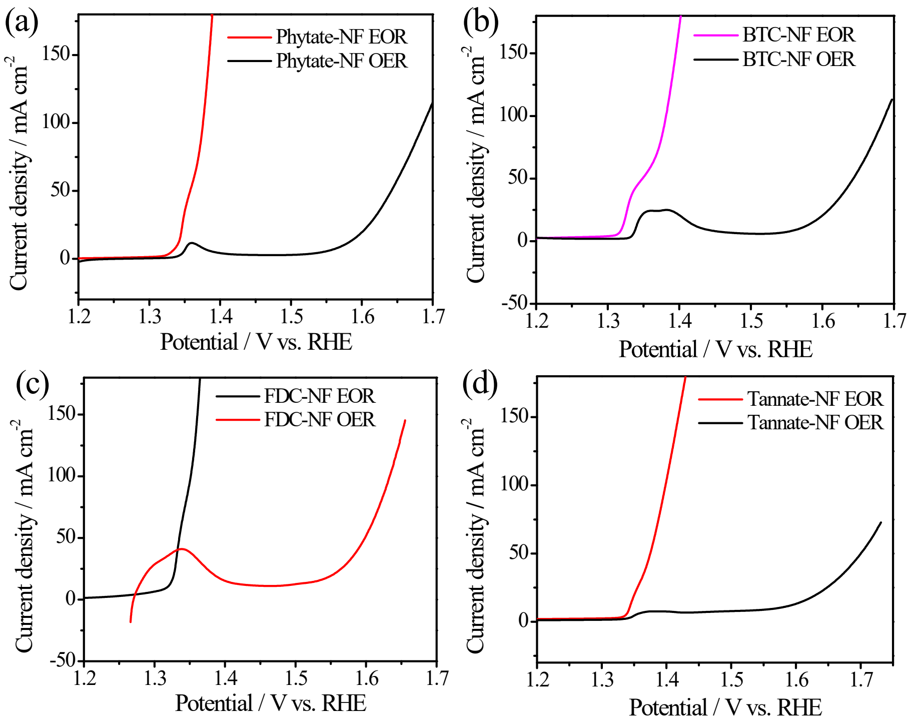

Fig. S7 LSV curves of EOR (in 1.0 mol L^{-1} KOH with 1.0 mol L^{-1} EtOH) and OER (in only 1.0 mol L^{-1} KOH) of (a) Phytate-NF, (b) BTC-NF, (c) FDC-NF and (d) Tannate-NF.

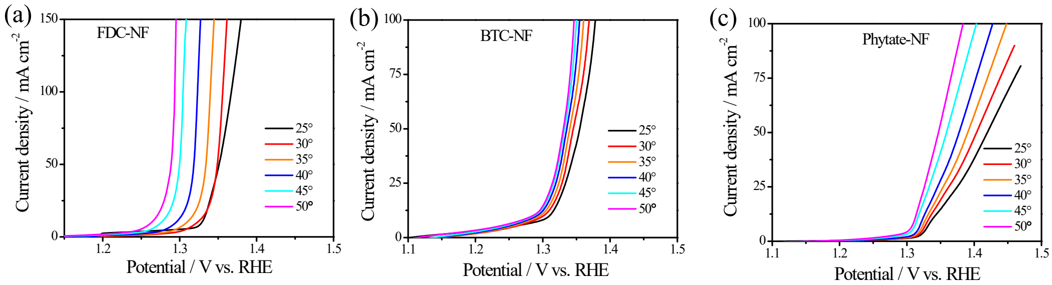

Fig. S8 LSV curves of (a) FDC-NF, (b) BTC-NF and (c) Phytate-NF at 25, 30, 35, 40, 45 and 50 °C.

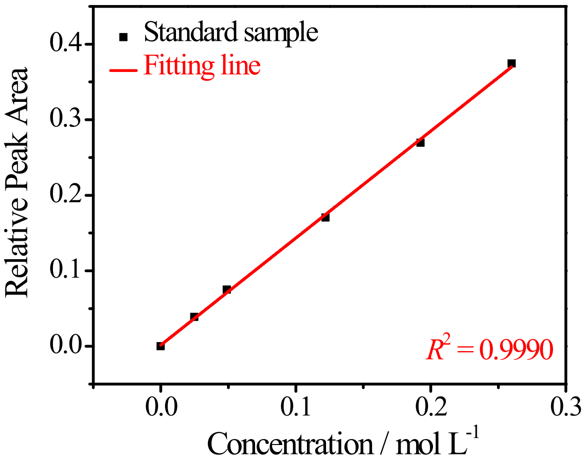

Fig. S9 Standard curve between acetic acid product at different concentration and the relative peak area in ^{1}H NMR.

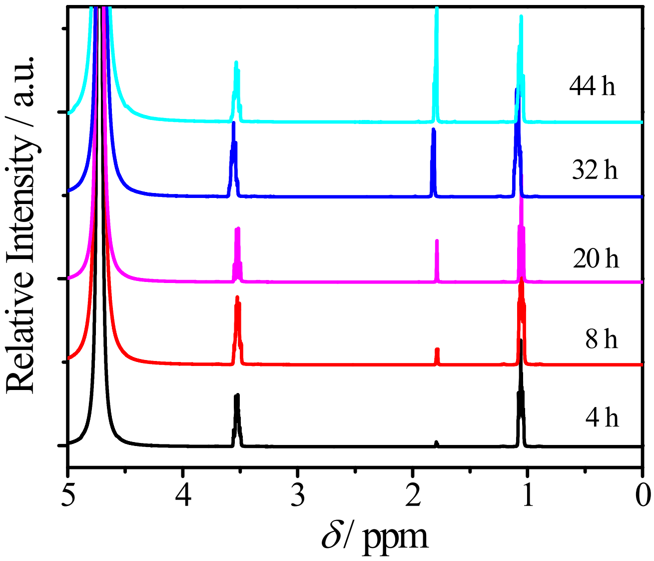

Fig. S10 ^{1}H NMR measurements of the products after chronopotentiometry test at 40 mA cm^{-2} for 4, 8, 20, 32 and 44 h on the FU-NF electrode.

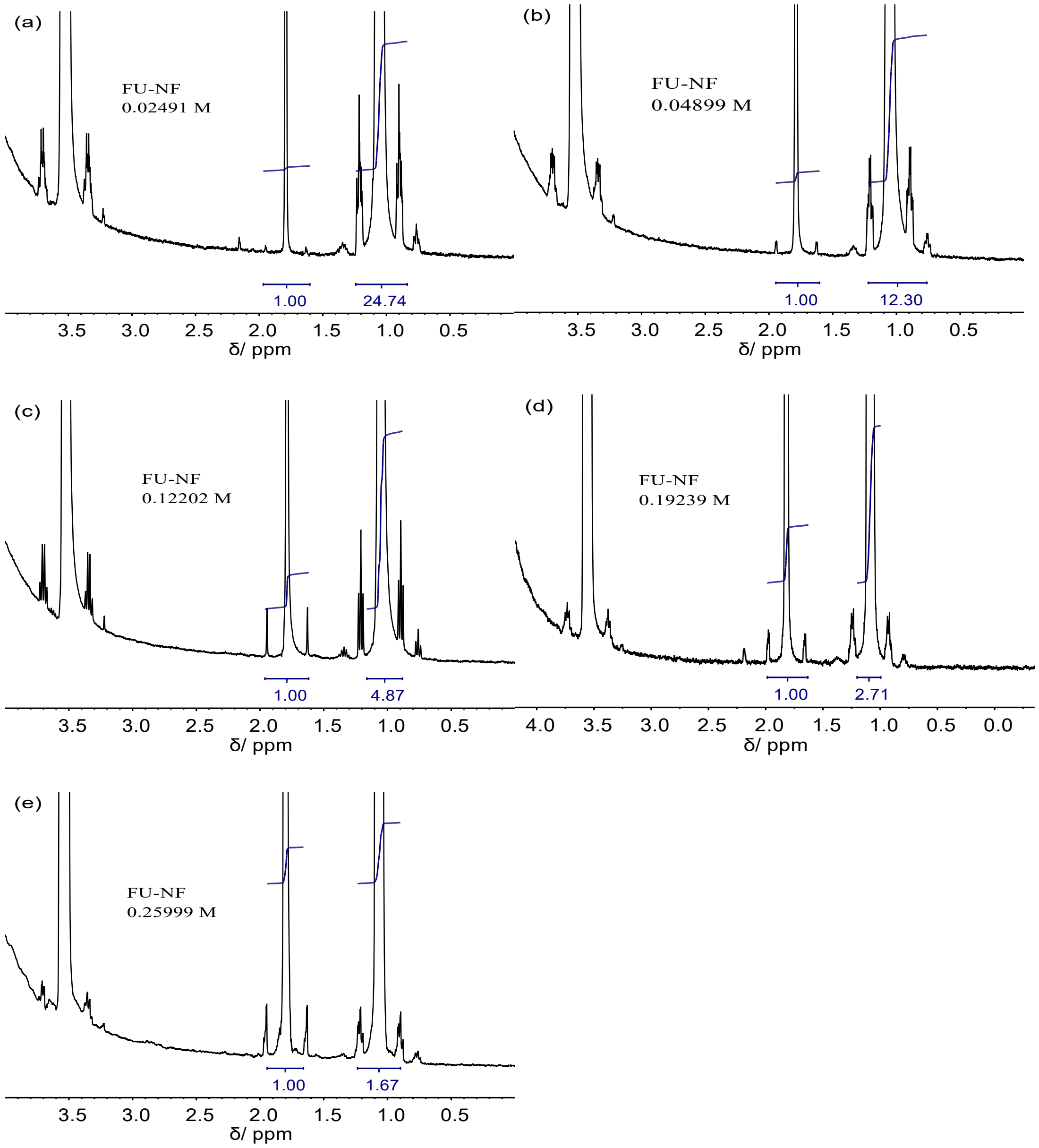

Fig. S11 ^{1}H NMR measurements of the products after chronopotentiometry test at 40 mA cm^{-2} for (a) 4 h, (b) 8 h, (c) 20 h, (d) 32 h and (e) 44 h on the FU-NF electrode.

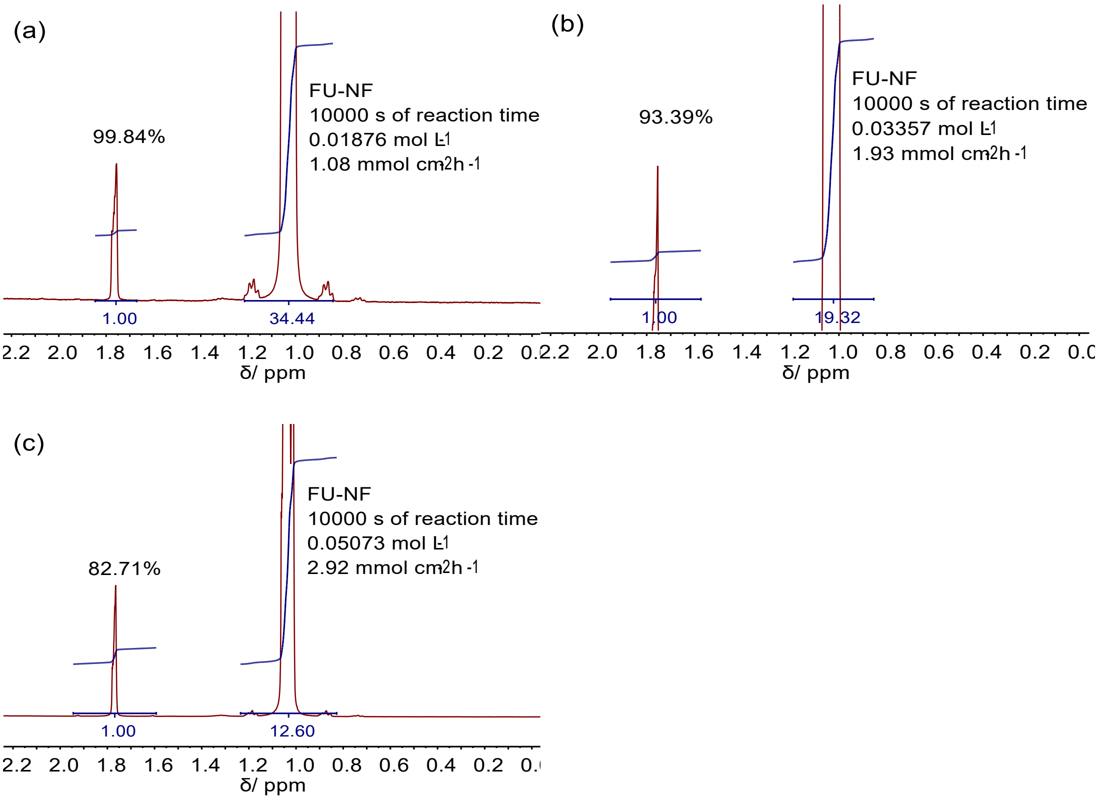

Fig. S12 Faradaic efficiency and acetate production rate for the reaction products obtained with the FU-NF electrode at (a) 1.4, (b) 1.5 and (c) 1.6 V_{RHE}.

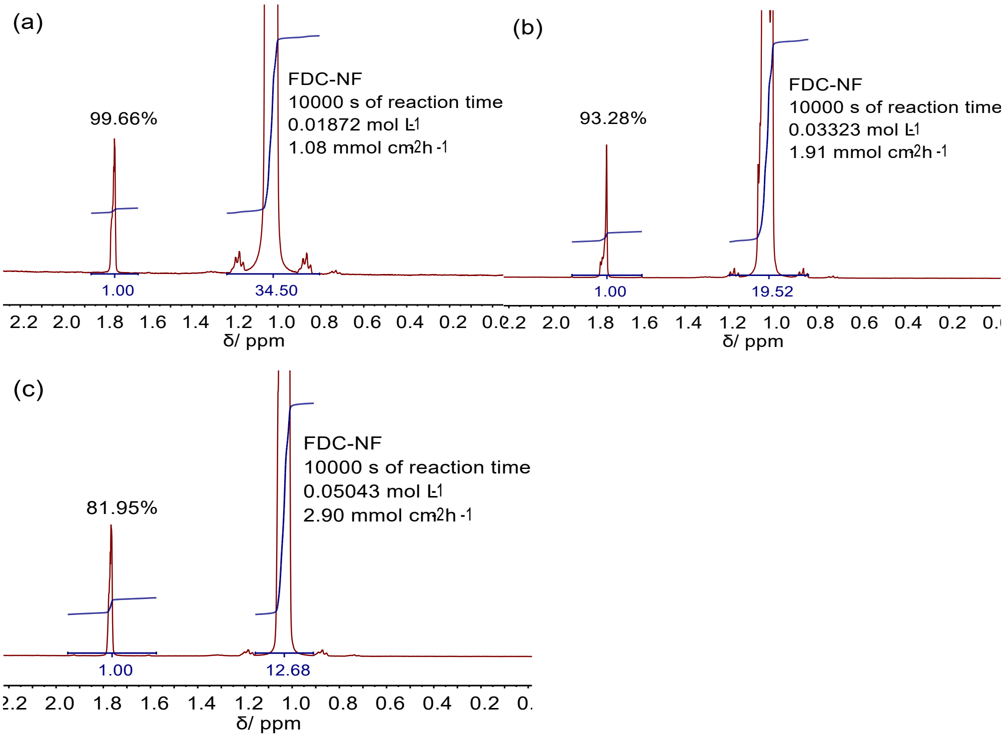

Fig. S13 Faradaic efficiency and acetate production rate for the reaction products obtained with the FDC-NF electrode at (a) 1.4, (b) 1.5 and (c) 1.6 V_{RHE}.

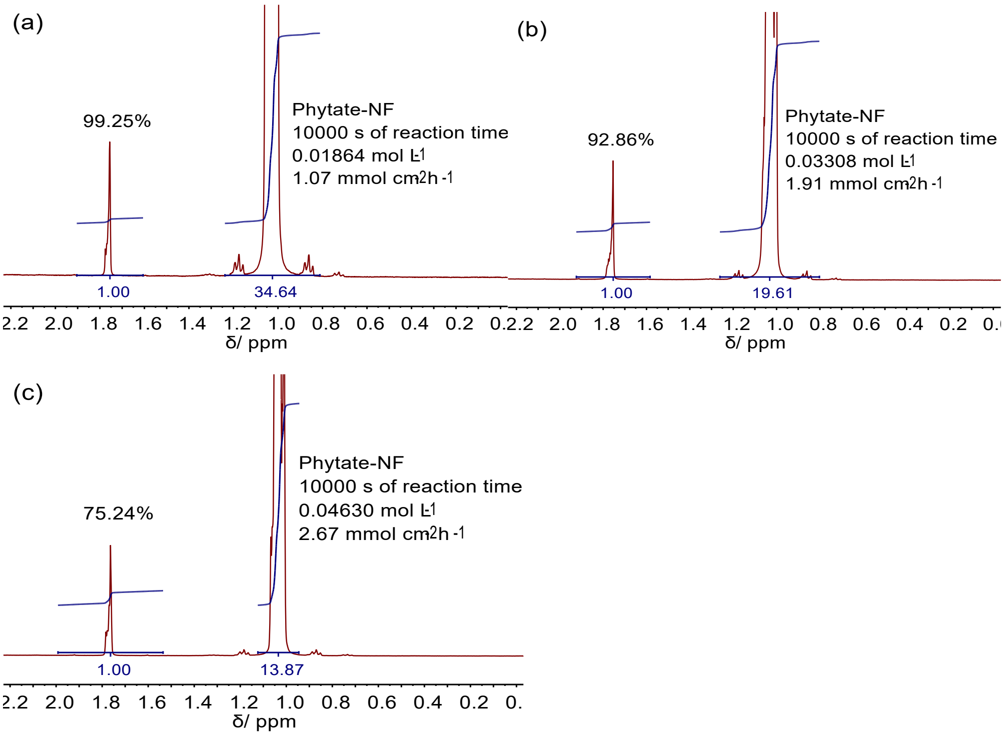

Fig. S14 Faradaic efficiency and acetate production rate for the reaction products obtained with the Phytate-NF electrode at (a) 1.4, (b) 1.5 and (c) 1.6 V_{RHE}.

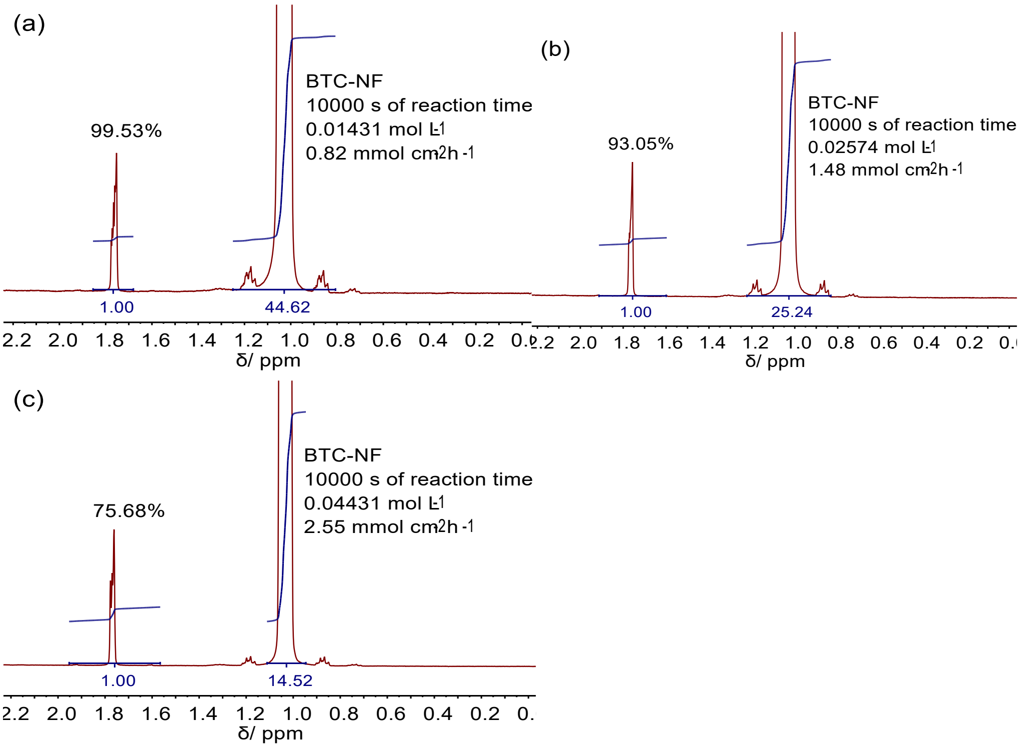

Fig. S15 Faradaic efficiency and acetate production rate for the reaction products obtained with the BTC-NF electrode at (a) 1.4, (b) 1.5 and (c) 1.6 V_{RHE}.

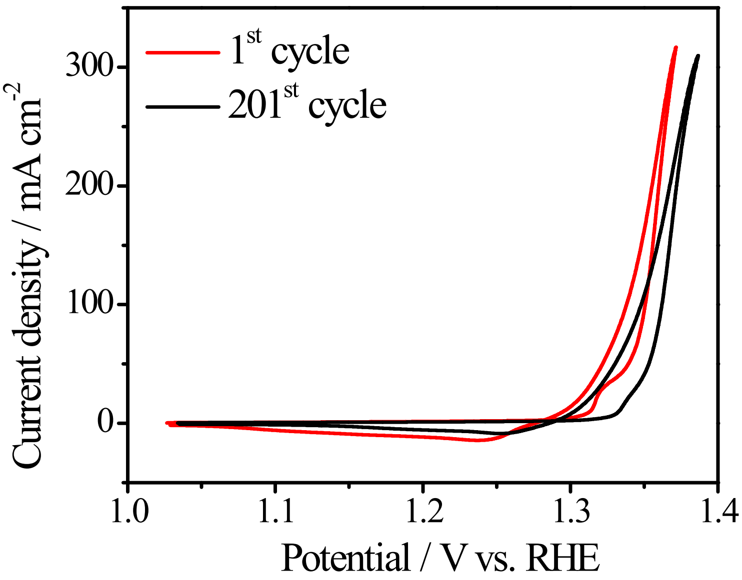

Fig. S16 CV cycling stability test of FU-NF at a scan rate of 50 mV s^{-1}.

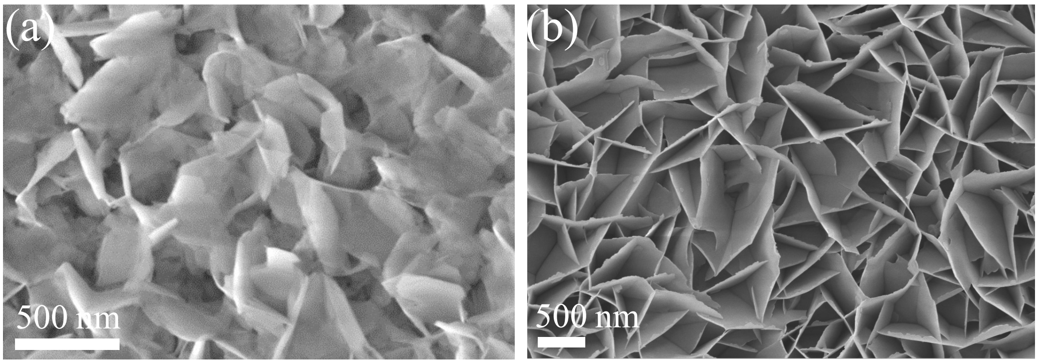

Fig. S17 SEM images of FU-NF (a) before and (b) after the long-term chronopotentiometric measurement at 1.5 V for 10000 s.

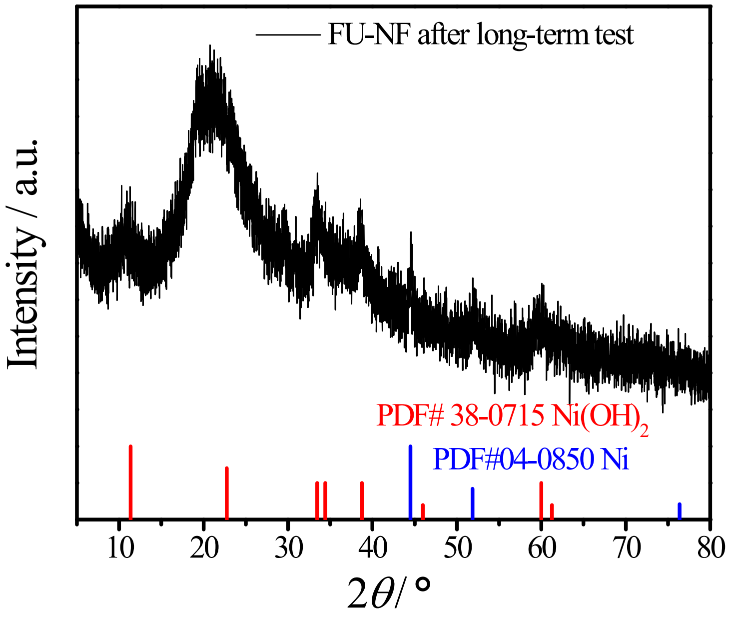

Fig. S18 XRD pattern of powder FU-NF after the long-term chronopotentiometric measurement at 1.5 V for 10000 s.

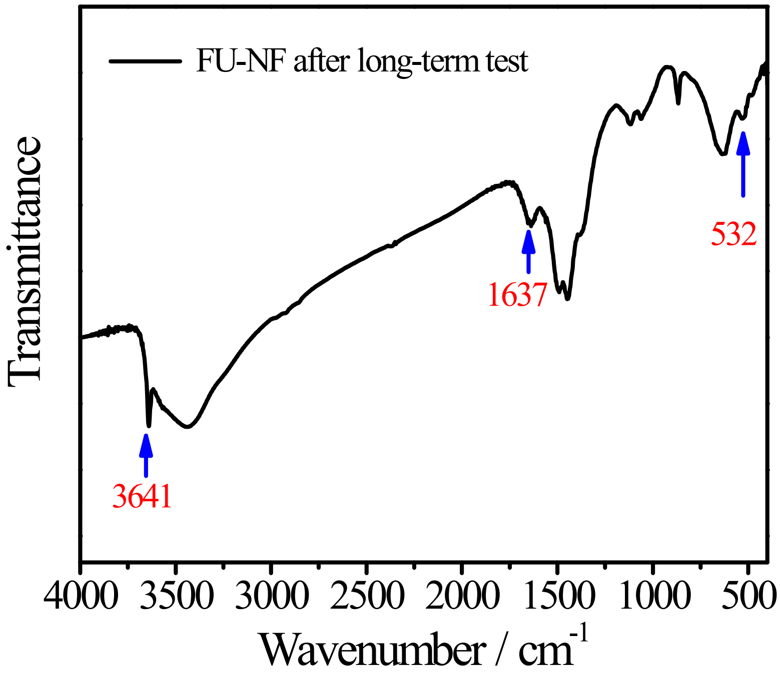

Fig. S19 FT-IR spectrum of powder FU-NF after the long-term chronopotentiometric measurement at 1.5 V for 10000 s.

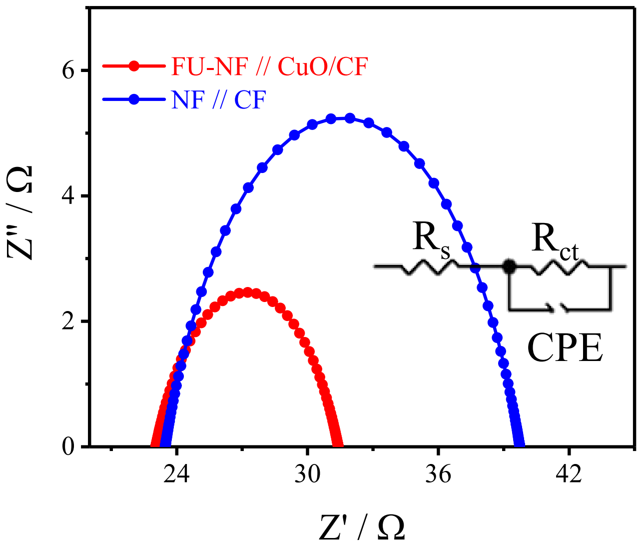

Fig. S20 Electrochemical impedance spectroscopy (EIS) analyses for FU-NF // CuO/CF and NF // CF at 1.4 V vs RHE (inset is the equivalent circuit).

Table S1 Comparison of the EOR performance of FU-NF electrode in terms of Tafel slope and potential at a current density of 100 mA cm^{-2} with some state-of-the-art Ni-based electrocatalysts.

Catalyst	Potential at 100 mA cm^{-2} / V	Tafel slope /mV dec^{-1}	Ref.
NiO@CeO$_2$	≈1.70	21	[55]
NiCo-LDHs	≈1.54	71.58	[56]
Co$_1$Ni$_{0.5}$Mn$_1$BDC@NF-A	1.30	31	[57]
NiOOH-CuO/CF	≈1.35	33.3	[39]
NiOOH@Co–NCO	1.340	31.3	[11]
Co(OH)$_2$@Ni(OH)$_2$	1.389	55	[19]
CO(NH$_2$)$_2$/NF	≈1.39	81.68	[33]
FU-NF	1.353	46.89	This work